INTERNATIONAL JOURNAL FOR NUMERICAL METHODS IN ENGINEERING
Int. J. Numer. Meth. Engng 2003; **03**:1–23

A Variationally Consistent Fractional Time Step Integration Method for Lagrangian Dynamics

Sudeep K. Lahiri [1], Javier Bonet [2], Jaime Peraire [1,*] and Lluis Casals [2]

[1] *Aerospace Computational Design Laboratory, Department of Aeronautics, MIT, Cambridge, USA.*
[2] *Civil & Computational Engineering Centre, School of Engineering, University of Wales, Swansea, UK.*

SUMMARY

In this paper we present a fractional time step method for Lagrangian formulations of solid dynamics problems. The method can be interpreted as belonging to the class of variational integrators which are designed to conserve linear and angular momentum of the entire mechanical system exactly. Energy fluctuations are found to be minimal and stay bounded for long durations.

In order to handle incompressibility, a mixed formulation in which the pressure appears explicitly is adopted. The velocity update over a time step is split into deviatoric and a volumetric components. The deviatoric component is advanced using explicit time marching, whereas the pressure correction for each time step, is computed implicitly by solving a Poisson-like equation. Once the pressure is known, the volumetric component of the velocity update is calculated. In contrast with standard explicit schemes, where the timestep size is determined by the speed of the pressure waves, the allowable timestep for the proposed scheme is found to depend only on the shear wave speed. This leads to a significant advantage in the case of nearly incompressible materials and permits the solution of truly incompressible problems.

KEY WORDS: Variational time integrators, Mixed formulation, Incompressibility.

1. INTRODUCTION

Dynamic problems involving rapid phenomena are encountered in many engineering applications. Generally, this type of problems are discretised in space using tri-linear hexahedral elements and integrated in time in a Lagrangian manner with an explicit leap-frog time stepping procedure. The resulting explicit integration is conditionally stable with a critical timestep given by the time that the volumetric wave takes to cross the smallest characteristic element length. Inevitably, for nearly incompressible materials the resulting timesteps are very small, specially in the presence of large distortions which often lead to very small characteristic

*Correspondence to: Jaime Peraire, Massachusetts Institute of Technology, Aerospace Computational Design Laboratory, MIT 37-461, Cambridge, MA 02139, USA

Contract/grant sponsor: Sandia National Laboratory, USA.; contract/grant number: Doc. No. 1152 under A0260

element sizes. Moreover, the fully incompressible limit cannot be modelled with these type of methods and consequently materials such as rubber or common fluids need to be approximated as nearly incompressible.

In Eulerian fluid dynamics, incompressible flows are often modelled using fractional time integration schemes [10], where the pressure is integrated in time in an implicit manner. Extending these ideas to solids in which the geometry is constantly changing requires introducing the pressure as an additional variable and has been attempted in [12] and [14] using linear tetrahedral elements. In both these references, however, the motivation for treating pressure as a problem variable was to eliminate the well-known problem of volumetric locking encountered by the standard linear triangular and tetrahedral elements. Unfortunately, the pressure step was taken explicitly and the resulting critical timestep is much smaller than that obtained with standard integration [14].

The aim of this paper is to present a fractional step integration for Lagrangian solid dynamic applications which is implicit in the pressure, or volumetric terms, but explicit for the deviatoric component. Previous researchers [17] have developed similar methods for solid dynamics using fully implicit schemes. Although such methods are unconditionally stable they become very expensive for large size problems. The scheme proposed here is formulated taking advantage of the recently proposed variational framework for time integrators described in references [3] [9] [4].

Variational integrators have been developed on the basis of Hamilton's Stationarity principle rather than discretising in time the differential equations of motion. Hamilton's principle dictates that the path followed by a body represents a stationary point of the integral of the Lagrangian over a given interval. Variational integrators take advantage of this principle by constructing a discrete approximation of this integral which then becomes a function of a finite number of positions of the body at each timestep. The stationary conditions of the resulting discrete functional with respect to each body configuration lead to time stepping algorithms that retain many of the conservation properties of the continuum problem. In particular, the schemes developed in this way satisfy exact preservation of linear and angular momentum and are simplectic [4]. In addition, these algorithms are found to have excellent energy conservation properties even though the exact reasons for this are not fully understood [4]. This class of variational algorithms includes both implicit and explicit schemes, and in particular, it includes some well-known members of the Newmark family.

In order to introduce a fractional procedure within the variational framework, the volumetric component of the internal energy will be expressed in a mixed form in terms of the geometry and pressure using the complementary volumetric energy. In addition, different approximations will be used for the isochoric and volumetric components of the integrated Lagrangian. In this way the velocity update over a time step is split into a deviatoric component and a volumetric component. The deviatoric component is advanced using explicit time marching, whereas the pressure correction for each time step is computed using an implicit time integration. Once the pressure is known, the volumetric component of the velocity update is calculated. This type of mixed formulation, relaxes the timestep restriction encountered in general explicit schemes. For linear cases it can be shown that the maximum time step that can be used only depends on the deviatoric wave speed of the material, which leads to a significant advantage in case of nearly incompressible material behavior and allows the fully incompressible limit to be modelled. The examples presented in the paper will indicate that this is also true for more general nonlinear applications.

Unfortunately, given the geometrical non-linearity inherent in the type of applications of interest, the resulting equations for the pressure are non-linear. Fortunately, this non-linearity can be easily eliminated if the volume increment over a timestep is calculated in an approximate manner using the divergence of the velocity. In this way a set of linear equations for the pressure is obtained at each step with a structure similar to that of a discrete Poisson solution.

The paper is organized as follows. Section 2 defines the Lagrangian function for the continuum problem, including the internal energy terms for simple neo-Hookean materials, and presents the Hamilton's principle as the variational principle governing the problem. Section 3 explains how the variational framework can be used to obtain time integrators that preserve the invariants of the motion. Section 4 uses the above framework to derive the fractional step algorithm proposed. Section 5 discusses the finite element discretisation and section 6 a linearised form of the volumetric equations that eliminates the need to solve a system of nonlinear equations at each step. Section 7 describes a linearised stability analysis which shows that the critical timestep of the proposed scheme is independent of the volumetric wave speed. Section 8 presents a number of examples that extend this conclusion to more general cases and section 9 summarizes the key aspects of the proposed method.

2. THE CONTINUOUS PROBLEM

We consider the motion under loading of a three dimensional body. We adopt a reference configuration, $Q \subset \mathcal{R}^3$, corresponding to the configuration of the body at time $t = 0$. The material coordinates $\boldsymbol{X} \in Q$, are used to label the particles of the body. At an arbitrary time t, the position of particle $\boldsymbol{X}$ is given by the coordinate $\boldsymbol{x}$, and in general, the motion of the body is described by a deformation mapping,

$$\boldsymbol{x} = \phi(\boldsymbol{X}, t), \tag{1}$$

as illustrated in figure 1. In its reference configuration, the body has volume V_0 and density ρ_0, whereas at a given time t, the body has volume $V(t)$ and density $\rho(t)$.

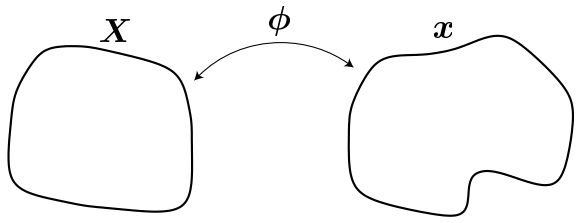

Figure 1. Continuous systems

2.1. The Action Integral for non-dissipative systems

For non-dissipative systems, both the internal and external forces in the system can be derived from a potential, and the motion between times $t_0 = 0$ and t, can be determine from Hamilton's principle. To this end, we introduce a Lagrangian, $\mathcal{L}$,

$$\mathcal{L}(\boldsymbol{x}, \dot{\boldsymbol{x}}) = \mathcal{K}(\dot{\boldsymbol{x}}) - \Pi(\boldsymbol{x}) \ ,$$

where, $\mathcal{K}$, denotes the kinetic energy, Π is the potential energy and $\dot{\boldsymbol{x}} = d\boldsymbol{x}/dt$ is the material velocity. The potential energy can be generally decomposed into an internal elastic component, Π_{int}, and a component accounting for the external conservative forces, Π_{ext}. Thus, $\Pi(\boldsymbol{x}) = \Pi_{\text{int}}(\boldsymbol{x}) + \Pi_{\text{ext}}(\boldsymbol{x})$. The action integral, S, is defined as the integral of the of the Lagrangian over the time interval considered,

$$S = \int_0^t \mathcal{L}\, dt \,, \tag{2}$$

and Hamilton's principle states that the deformation mapping satisfying the equations of motion can be obtained by making the action integral stationary with respect to all possible deformation mappings which are compatible with the boundary conditions.

2.2. The Kinetic Energy, $(\mathcal{K})$

The kinetic energy of the body is a function of the velocity and can be written as,

$$\mathcal{K}(\dot{\boldsymbol{x}}) = \int_{V_0} \frac{1}{2}\rho_0 \dot{\boldsymbol{x}}^2\, dV_0 \,.$$

2.3. The Internal Potential Energy (Π_{int})

The internal potential energy depends on the constitutive relations of the materials in our system. In this paper we shall consider hyperelastic Neo-Hookean materials undergoing large deformations and displacements.
Let $\boldsymbol{F}$ be the deformation gradient tensor which can be written as,

$$\boldsymbol{F}_{ij} = \frac{\partial x_i}{\partial X_j} \qquad \forall\ i,j = 1,..,3$$

The relevant kinematic quantities associated with the deformation gradient are the right Cauchy-Green tensor, $\boldsymbol{C}$, the Jacobian, J, and the deviatoric component of $\boldsymbol{C}$, $\hat{\boldsymbol{C}}$, which are given by,

$$\boldsymbol{C} = \boldsymbol{F}^T\boldsymbol{F}; \qquad J = \det(\boldsymbol{F}); \qquad \hat{\boldsymbol{C}} = J^{-\frac{2}{3}}\boldsymbol{C} \,.$$

For isotropic Neo-Hookean materials, the internal potential energy can be expressed in terms of the Lame constant μ, and the bulk modulus κ as

$$\Pi_{\text{int}}(\boldsymbol{x}) = \int_V \left[\frac{\mu}{2}\left(tr(\hat{\boldsymbol{C}}) - 3\right) + \frac{1}{2}\kappa(J-1)^2\right] dV_0 \,. \tag{3}$$

The above expression is well suited for compressible or nearly incompressible materials. However, when the material approaches incompressibility, the bulk modulus, κ, becomes very large and this causes $\Pi_{\text{int}}(\boldsymbol{x})$, in (3), to be unbounded for all motions not satisfying $J = 1$. This is a constraint on the allowable deformations which, in practice, is difficult to enforce a priori. A more suitable formulation which still allows us to work with general motions is obtained by introducing the constraint, $J = 1$, through a Lagrange multiplier. It turns out that, it is actually possible to reformulate the internal potential energy, by introducing an additional pressure variable in such a way that a formulation which is valid for both compressible and incompressible materials is obtained. In the compressible case, the pressure can be determined

from the volumetric change as $p = \kappa(J-1)$, whereas in the incompressible limit, the pressurte becomes a Lagrange multiplier which enforces $J = 1$. We write,

$$\Pi_{\text{int}}(\boldsymbol{x}, p) \quad = \quad \Pi_{\text{iso}}(\boldsymbol{x}) + \Pi_{\text{vol}}(\boldsymbol{x}, p) \ , \tag{4}$$

where,

$$\Pi_{\text{iso}}(\boldsymbol{x}) \quad = \quad \int_{V_0} \frac{\mu}{2}(tr(\hat{\boldsymbol{C}}) - 3)\, dV_0 \ , \tag{5}$$

and,

$$\Pi_{\text{vol}}(\boldsymbol{x}, p) \quad = \quad \int_{V_0} p(J-1) dV_0 - \int_{V_0} \frac{p^2}{2\kappa}\, dV_0 \ . \tag{6}$$

For compressible materials, the constitutive equation relating the volumetric changes and the pressure is recovered by setting the variation of Π_{vol} with respect to p equal to zero. Thus the form (4-6) of the internal potential function, has the property that it is equivalent to the irreducible form (3), but as the material becomes incompressible, the second term in Π_{vol} disappears and only the constraint times the lagrange multiplier, p, remains. As expected, for incompressible materials, $\Pi_{\text{vol}} \to 0$, and $\Pi_{\text{iso}} \to \Pi_{\text{int}}$. It is clear that when we adopt the form (4-6) for the internal potential energy, the Lagrangian will also depend on the pressure, that is $\mathcal{L}(\boldsymbol{x}, \dot{\boldsymbol{x}}, p)$, and that the solution will need to be determined by requiring stationarity of the action integral, (2), with respect to $\boldsymbol{x}$ and p.

2.4. The External Potential Energy (Π_{ext})

The external potential energy includes the work done by the external body and surface forces.

$$\Pi_{\text{ext}}(\boldsymbol{x}) \quad = \quad \int_{V_0} \boldsymbol{f}^b \cdot \boldsymbol{x}\, dV_0 + \int_{\partial V_0} \boldsymbol{f}^s \cdot \boldsymbol{x}\, dS_0 \ .$$

Here, $\boldsymbol{f}^b$ are the body forces, $\boldsymbol{f}^s$ are the surface forces, and ∂V_0 denotes the section of the boundary, in the reference configuration, where the surface forces are applied.

3. TIME INTEGRATION

3.1. Variational Formulation

Consider now a sequence of timesteps $t_{n+1} = t_n + \Delta t,\ n = 0, 1, ..., N$, where for simplicity a constant step size has been taken. The position of the body at each step is defined by a mapping $\boldsymbol{x}_n = \phi(\boldsymbol{X}, t_n)$. A variational algorithm is defined by a discrete sum integral,

$$S(\boldsymbol{x}_0, \boldsymbol{x}_1, ..., \boldsymbol{x}_N) \approx \sum_{n=0}^{N-1} L_{n,n+1}(\boldsymbol{x}_n, \boldsymbol{x}_{n+1}) \ ,$$

where the discrete Lagrangian L approximates the integral of the continuum Lagrangian $\mathcal{L}$ over a timestep, that is,

$$L_{n,n+1}(\boldsymbol{x}_n, \boldsymbol{x}_{n+1}) \approx \int_{t_n}^{t_{n+1}} \mathcal{L}(\boldsymbol{x}, \dot{\boldsymbol{x}})\, dt \ . \tag{7}$$

Here, for simplicity, we consider the case in which the Lagrangian is a function of $\boldsymbol{x}$ and $\dot{\boldsymbol{x}}$ only. The pressure variable will be introduced later. Obviously, there are a number of ways in which the approximation (7) can be chosen, and, as we shall see, each one will lead to a different time integration algorithm.

The stationary conditions of the discrete sum integral S with respect to a variation $\delta \boldsymbol{v}_n$ of the body position at time step n are now given by,

$$D_n S[\delta \boldsymbol{v}_n] = D_2 L_{n-1,n}(\boldsymbol{x}_{n-1}, \boldsymbol{x}_n)[\delta \boldsymbol{v}_n] + D_1 L_{n,n+1}(\boldsymbol{x}_n, \boldsymbol{x}_{n+1})[\delta \boldsymbol{v}_n] = 0 \qquad \forall \delta \boldsymbol{v}_n \ , \tag{8}$$

where D_i denotes directional derivative with respect to i-th variable. The above equation represents the statement of equilibrium at step n and will enable the positions at step $n+1$ to be evaluated in terms of positions at $n-1$ and n. It will be shown in the next section that regardless of the actual discrete Lagrangian chosen, the algorithms derived following the above variational procedure will inherit the conservation properties of the continuum system. Moreover, it is also shown in [4] that this type of algorithms are also simplectic.

As a simple example of the above variational integrators, consider first the standard case of the commonly used central difference (or leap-frog) time integrator. This well-known scheme is arrived at by defining the discrete Lagrangian between two timesteps as,

$$L_{n,n+1}(\boldsymbol{x}_n, \boldsymbol{x}_{n+1}) = \frac{\Delta t}{2} M(\boldsymbol{v}_{n+1/2}, \boldsymbol{v}_{n+1/2}) - \Delta t \, \Pi(\boldsymbol{x}_n) \ , \tag{9}$$

where the intermediate velocity is defined as $\boldsymbol{v}_{n+1/2} = (\boldsymbol{x}_{n+1} - \boldsymbol{x}_n)/\Delta t$ and the mass bilinear form is given by,

$$M(\boldsymbol{u}, \boldsymbol{v}) = \int_{V_0} (\boldsymbol{u} \cdot \boldsymbol{v}) \, \rho_0 \, dV_0 \ . \tag{10}$$

Substituting into equation (8) for the above discrete Lagrangian expression leads, after some simple algebra, to the standard explicit central difference time integration scheme,

$$M\left(\delta \boldsymbol{v}_n, \frac{\boldsymbol{v}_{n+1/2} - \boldsymbol{v}_{n-1/2}}{\Delta t}\right) = F(\delta \boldsymbol{v}_n; \boldsymbol{x}_n) - T(\delta \boldsymbol{v}_n; \boldsymbol{x}_n) \ , \tag{11}$$

where the external and internal forces are respectively,

$$\begin{aligned} F(\delta \boldsymbol{v}; \boldsymbol{x}_n) &= -D\Pi_{\text{ext}}(\boldsymbol{x}_n)[\delta \boldsymbol{v}] \ , \\ T(\delta \boldsymbol{v}; \boldsymbol{x}_n) &= D\Pi_{\text{int}}(\boldsymbol{x}_n)[\delta \boldsymbol{v}] \ . \end{aligned} \tag{12}$$

Remark For a uniform step size, identical explicit equations are in fact obtained if the Lagrangian is approximated as,

$$L_{n,n+1}(\boldsymbol{x}_n, \boldsymbol{x}_{n+1}) = \frac{\Delta t}{2} M(\boldsymbol{v}_{n+1/2}, \boldsymbol{v}_{n+1/2}) - \Delta t \, \Pi(\boldsymbol{x}_{n+1}) \ , \tag{13}$$

or indeed,

$$L_{n,n+1}(\boldsymbol{x}_n, \boldsymbol{x}_{n+1}) = \frac{\Delta t}{2} M(\boldsymbol{v}_{n+1/2}, \boldsymbol{v}_{n+1/2}) - \frac{\Delta t}{2} \Pi(\boldsymbol{x}_n) - \frac{\Delta t}{2} \Pi(\boldsymbol{x}_{n+1}) \ . \tag{14}$$

However, for variable timestep size, only the last equation leads to the standard second order leap-frog scheme.

A different scheme, namely the mid-point rule, can be derived from an incremental Lagrangian defined as,

$$L_{n,n+1}(\boldsymbol{x}_n, \boldsymbol{x}_{n+1}) = \frac{\Delta t}{2} M(\boldsymbol{v}_{n+1/2}, \boldsymbol{v}_{n+1/2}) - \Delta t\, \Pi(\boldsymbol{x}_{n+1/2}); \qquad \boldsymbol{x}_{n+1/2} = \frac{1}{2}(\boldsymbol{x}_n + \boldsymbol{x}_{n+1}) \ . \tag{15}$$

Simple algebra shows that the resulting equilibrium equations are,

$$\begin{aligned} M\left(\delta \boldsymbol{v}_n, \frac{\boldsymbol{v}_{n+1/2} - \boldsymbol{v}_{n-1/2}}{\Delta t}\right) &= \frac{1}{2}\left\{F(\delta \boldsymbol{v}_n; \boldsymbol{x}_{n+1/2}) + F(\delta \boldsymbol{v}_n; \boldsymbol{x}_{n-1/2})\right. \\ &\quad \left. -T(\delta \boldsymbol{v}_n; \boldsymbol{x}_{n+1/2}) - T(\delta \boldsymbol{v}_n; \boldsymbol{x}_{n-1/2})\right\} \end{aligned} \tag{16}$$

This is clearly an implicit scheme. It is well known, however, that for the linear case it is unconditionally stable. Note also that the mid-point rule is more commonly written in a one step for as,

$$M\left(\delta \boldsymbol{v}_n, \frac{\boldsymbol{v}_{n+1} - \boldsymbol{v}_n}{\Delta t}\right) = F(\delta \boldsymbol{v}_n; \boldsymbol{x}_{n+\frac{1}{2}}) - T(\delta \boldsymbol{v}_n; \boldsymbol{x}_{n+\frac{1}{2}}); \qquad \boldsymbol{x}_{n+1} = \boldsymbol{x}_n + \tfrac{\Delta t}{2}(\boldsymbol{v}_n + \boldsymbol{v}_{n+1}) \ . \tag{17}$$

Averaging this expression written between n and $n+1$, and $n-1$ and n, it is easy to show that equation (16) is recovered.

3.2. Conservation of System Invariants

The conservation properties of the above variational algorithms are a consequence of the invariance of the Lagrangian with respect to rigid body translation and rotations. This is simply a particular case of Noether's Theorem, whereby the symmetries of the Lagrangian lead to preserved quantities throughout the motion [19].

Consider the case of linear momentum first. This easily follows from the translational invariance of the discrete Lagrangian in the absence of external forces. To show this note first that if there are no external forces, then for any arbitrary constant vector $\boldsymbol{a} \in \mathcal{R}^3$,

$$L_{n,n+1}(\boldsymbol{x}_n + \boldsymbol{a}, \boldsymbol{x}_{n+1} + \boldsymbol{a}) = L_{n,n+1}(\boldsymbol{x}_n, \boldsymbol{x}_{n+1}) \ .$$

Differentiating this expression gives,

$$D_1 L_{n,n+1}(\boldsymbol{x}_n, \boldsymbol{x}_{n+1})[\boldsymbol{a}] + D_2 L_{n,n+1}(\boldsymbol{x}_n, \boldsymbol{x}_{n+1})[\boldsymbol{a}] = 0 \ . \tag{18}$$

But from the equilibrium equation (8), taking $\delta \boldsymbol{v}_n = \boldsymbol{a}$, we obtain,

$$D_1 L_{n,n+1}(\boldsymbol{x}_n, \boldsymbol{x}_{n+1})[\boldsymbol{a}] = -D_2 L_{n,n+1}(\boldsymbol{x}_{n-1}, \boldsymbol{x}_n)[\boldsymbol{a}] \ .$$

Substituting into (18) gives,

$$D_2 L_{n,n+1}(\boldsymbol{x}_n, \boldsymbol{x}_{n+1})[\boldsymbol{a}] = D_2 L_{n,n+1}(\boldsymbol{x}_{n-1}, \boldsymbol{x}_n)[\boldsymbol{a}] \ , \tag{19}$$

which implies the preservation of the discrete linear momentum, $\boldsymbol{G}(\boldsymbol{x}_n, \boldsymbol{x}_{n+1})$, which is defined as,

$$\boldsymbol{G}(\boldsymbol{x}_n, \boldsymbol{x}_{n+1}) \cdot \boldsymbol{a} = D_2 L_{n,n+1}(\boldsymbol{x}_n, \boldsymbol{x}_{n+1})[\boldsymbol{a}] \qquad \forall\, \boldsymbol{a} \in \mathcal{R}^3 \ .$$

The case of angular momentum is similarly obtained from the invariance of the Lagrangian with respect to rotations,

$$L_{n,n+1}(\boldsymbol{R}\boldsymbol{x}_n, \boldsymbol{R}\boldsymbol{x}_{n+1}) \quad = \quad L_{n,n+1}(\boldsymbol{x}_n, \boldsymbol{x}_{n+1}) \tag{20}$$

where $\boldsymbol{R}$ is an orthogonal rotation matrix. Differentiating this expression now gives,

$$D_1 L_{n,n+1}(\boldsymbol{x}_n, \boldsymbol{x}_{n+1})[\boldsymbol{w} \times \boldsymbol{x}_n] + D_2 L_{n,n+1}(\boldsymbol{x}_n, \boldsymbol{x}_{n+1})[\boldsymbol{w} \times \boldsymbol{x}_{n+1}] \quad = \quad 0 \qquad \forall\, \boldsymbol{w} \in \mathcal{R}^3 \tag{21}$$

where $\boldsymbol{w}$ represents a small rotation (spin) vector associated with $\boldsymbol{R}$ which is arbitrary since the choice of $\boldsymbol{R}$, in (20), was also arbitrary. Again from (8) for the particular case $\delta \boldsymbol{v}_n = \boldsymbol{w} \times \boldsymbol{x}_n$ we obtain

$$D_1 L_{n,n+1}(\boldsymbol{x}_n, \boldsymbol{x}_{n+1})[\boldsymbol{w} \times \boldsymbol{x}_n] \quad = \quad -D_2 L_{n,n+1}(\boldsymbol{x}_{n-1}, \boldsymbol{x}_n)[\boldsymbol{w} \times \boldsymbol{x}_n] \;,$$

and substituting into equation (21) gives,

$$D_2 L_{n,n+1}(\boldsymbol{x}_n, \boldsymbol{x}_{n+1})[\boldsymbol{w} \times \boldsymbol{x}_{n+1}] \quad = \quad D_2 L_{n,n+1}(\boldsymbol{x}_{n-1}, \boldsymbol{x}_n)[\boldsymbol{w} \times \boldsymbol{x}_n] \;, \tag{22}$$

which leads to the following definition of the discrete angular momentum $\boldsymbol{H}(\boldsymbol{x}_n, \boldsymbol{x}_{n+1})$,

$$\boldsymbol{H}(\boldsymbol{x}_n, \boldsymbol{x}_{n+1}) \cdot \boldsymbol{w} \quad = \quad D_2 L_{n,n+1}(\boldsymbol{x}_n, \boldsymbol{x}_{n+1})[\boldsymbol{w} \times \boldsymbol{x}_{n+1}] \;. \tag{23}$$

Note that in order to define the discrete linear and angular momentum, only the dependence of the Lagrangian on the geometry is relevant. In particular, when the Lagrangian depends explicitly on geometry and the pressure, as in the next section, the above definitions and derivations remain unaffected.

As an illustration of the conservation laws derived above, consider the simple case of a system of particles with masses m^a for $a = 1, .., M$ as shown in figure 2. The configuration

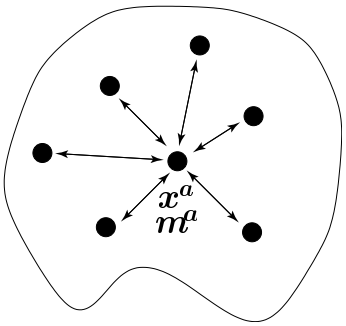

Figure 2. A system of particles

at time t_n is given by a vector $\boldsymbol{x}_n \in R^{3M}$ and $\mathbf{x}_n^T = [\boldsymbol{x}_n^1, \ldots, \boldsymbol{x}_n^a, \ldots]$. Consider the discrete Lagrangian,

$$L_{n,n+1}(\mathbf{x}_n, \mathbf{x}_{n+1}) \quad = \quad \sum_{a=1}^{M} \frac{\Delta t}{2} m^a \, \boldsymbol{v}_{n+1/2}^a \cdot \boldsymbol{v}_{n+1/2}^a - \Delta t \, \Pi(\mathbf{x}_n) \;, \tag{24}$$

where Π represents some internal potential leading to particle interaction forces (which is typically only a function of particle distances) and $\boldsymbol{v}^a_{n+1/2} = (\boldsymbol{x}^a_{n+1} - \boldsymbol{x}^a_n)/\Delta t$. Both linear and angular momentum emerge from,

$$D_2 L(\mathbf{x}_n, \mathbf{x}_{n+1})[\delta \mathbf{v}_{n+1}] \;=\; \sum_a m^a \, \boldsymbol{v}^a_{n+1/2} \cdot \delta \boldsymbol{v}^a_{n+1} \; . \tag{25}$$

For instance, taking $\delta \boldsymbol{v}^a_{n+1} = \boldsymbol{a}$, the standard definition of the linear momentum is recovered,

$$\boldsymbol{G}(\mathbf{x}_n, \mathbf{x}_{n+1}) \;=\; \sum_{a=1}^{M} m^a \, \boldsymbol{v}^a_{n+1/2} \; . \tag{26}$$

Taking $\delta \boldsymbol{v}^a_{n+1} = \boldsymbol{w} \times \boldsymbol{x}^a_{n+1}$ gives, after some trivial algebra, the angular momentum as

$$\boldsymbol{H}(\mathbf{x}_n, \mathbf{x}_{n+1}) \;=\; \sum_{a=1}^{M} m^a \, \boldsymbol{x}^a_{n+1} \times \boldsymbol{v}^a_{n+1/2} \; . \tag{27}$$

Note that if we consider a finite element discretization with a lumped mass matrix, the expressions for the discrete linear an angular momentuim of the system are analogous to (26, 27).

4. FRACTIONAL STEP VARIATIONAL FORMULATION

Here, we extend the time integration algorithms introduced in the previous section to the case in which the volumetric internal potential energy, and in turn the Lagrangian, is expressed in terms of the configuration $\boldsymbol{x}$, and the pressure, p, as given by equations (4-6).
We consider the following discrete Lagrangian between any two steps n and $n+1$,

$$\begin{aligned} L_{n,n+1}(\boldsymbol{x}_n, \boldsymbol{x}_{n+1}, p_{n+\frac{1}{2}}) \;=\; & \frac{1}{2} M(\boldsymbol{v}_{n+1/2}, \boldsymbol{v}_{n+1/2}) - \Pi_{\text{iso}}(\boldsymbol{x}_n) - \Pi_{\text{ext}}(\boldsymbol{x}_n) \\ & - \int_{V_0} \frac{1}{2} p_{n+1/2} (J_{n+1} + J_n - 2) \, dV_0 + \int_{V_0} \frac{p^2_{n+1/2}}{2\kappa} \, dV_0 \end{aligned} \tag{28}$$

Note that a central difference approximation for the volumetric components has been used and that we have chosen to evaluate the pressure at the half step. The stationary conditions of the action integral with respect to position at step n can now be obtained with the help of the expression $DJ[\delta \boldsymbol{v}] = J \text{div} \delta \boldsymbol{v}$, and lead to,

$$M\left(\delta \boldsymbol{v}_n, \frac{\boldsymbol{v}_{n+1/2} - \boldsymbol{v}_{n-1/2}}{\Delta t}\right) = F(\delta \boldsymbol{v}_n; \boldsymbol{x}_n) - T'(\delta \boldsymbol{v}_n; \boldsymbol{x}_n) - \int_{V_n} \frac{1}{2} (p_{n-1/2} + p_{n+1/2}) \, \text{div} \delta \boldsymbol{v}_n \, dV_n \tag{29}$$

where $T'(\delta \boldsymbol{v}; \boldsymbol{x}) = D\Pi_{\text{iso}}(\boldsymbol{x}_n)[\delta \boldsymbol{v}]$ represents the isochoric, or deviatoric, component of the internal forces, and the domain of integration has been changed from V_0 to that in the configuration at time level n, V_n, noting that $dV_0 = J_n dV_n$. Note also that the divergence of $\delta \boldsymbol{v}_n$ is taken at the current configuration n. Introducing the additional velocity variable, $\boldsymbol{v}^*_{n+1/2}$, the above expression can now be re-arranged in a more traditional fractional step format as,

$$M\left(\delta \boldsymbol{v}_n, \frac{\boldsymbol{v}^*_{n+1/2} - \boldsymbol{v}_{n-1/2}}{\Delta t}\right) = F(\delta \boldsymbol{v}_n; \boldsymbol{x}_n) - T'(\delta \boldsymbol{v}_n; \boldsymbol{x}_n) - \frac{1}{2} \int_{V_n} p_{n-1/2} \, \text{div} \delta \boldsymbol{v}_n \, dV_n \; , \tag{30}$$

$$M\left(\delta \boldsymbol{v}_n, \frac{\boldsymbol{v}_{n+1/2} - \boldsymbol{v}^*_{n+1/2}}{\Delta t}\right) = -\frac{1}{2}\int_{V_n} p_{n+1/2}\, \mathrm{div}\delta \boldsymbol{v}_n \, dV_n \ . \tag{31}$$

Assuming $\boldsymbol{x}_n$, $\boldsymbol{x}_{n+1}$ and $p_{n-1/2}$ are known, $\boldsymbol{v}^*_{n+1/2}$ can be determined explicitly from the first equation. However, the computation of $\boldsymbol{v}_{n+1/2}$ from the second equation, requires the solution of an additional equation for $p_{n+1/2}$. This equation is derived from the stationarity condition of the action integral with respect to the pressure. This gives,

$$M_\kappa(\delta p, p_{n+1/2}) = \int_{V_0} \frac{1}{2}(J_n + J_{n+1} - 2)\delta p \, dV_0 \tag{32}$$

where the notation

$$M_\kappa(p, q) = \int_{V_0} \frac{1}{\kappa} p\, q \, dV_0 \ ,$$

has been used. Note that for incompressible materials $\kappa \to \infty$ and the above expression enforces that the average volume ratio should be one.

The combined solution of equations (32) and (31) is described below in the context of a finite element discretization.

5. FINITE ELEMENT SPATIAL DISCRETIZATION

Consider now a standard linear tetrahedral finite element space consisting of M nodes for both the pressure and geometry of the solid. The finite dimensional approximations p_h and $\boldsymbol{x}_h$, are given by,

$$p_h = \sum_{a=1}^{M} N^a(\boldsymbol{X})\, p^a_h \qquad ; \qquad \boldsymbol{x}_h = \sum_{a=1}^{M} N^a(\boldsymbol{X})\, \boldsymbol{x}^a_h \ . \tag{33}$$

The discretization of equations (30) and (31) is expressed as,

$$\mathbf{M}\frac{\mathbf{v}^*_{n+1/2} - \mathbf{v}_{n-1/2}}{\Delta t} = \mathbf{F}_n - \mathbf{T}'_n - \frac{1}{2}\mathbf{G}_n \mathbf{p}_{n-1/2} \tag{34}$$

$$\mathbf{M}\frac{\mathbf{v}_{n+1/2} - \mathbf{v}^*_{n+1/2}}{\Delta t} = -\frac{1}{2}\mathbf{G}_n \mathbf{p}_{n+\frac{1}{2}} \tag{35}$$

where $\mathbf{M}$ is the mass matrix, $\mathbf{F}$ the vector of external forces, $\mathbf{T}'$ are the equivalent internal forces due to the deviatoric component of the stress, $\mathbf{v}^T_{n+1/2} = [\boldsymbol{v}^1_{h,n+1/2}, \ldots \boldsymbol{v}^a_{h,n+1/2}, \ldots]$ (with $\boldsymbol{v}^a_{h,n+1/2} = (\boldsymbol{x}^a_{h,n+1} - \boldsymbol{x}^a_{h,n})/\Delta t$) are the nodal velocities, $\mathbf{p}^T = [p^1_h, \ldots p^a_h, \ldots]$ the nodal pressures and the gradient-like matrix at time level n, $\mathbf{G}_n$, has nodal components $[\mathbf{G}]^{ab}_n$ given by,

$$[\mathbf{G}]^{ab}_n = \int_{V_n} N^b \nabla_n N^a \, dV_n \ . \tag{36}$$

Note that the weighting functions in expression (34) corresponding to the velocity degrees of freedom which are prescribed by boundary conditions are set to zero. As a result all the entries in the row of $\mathbf{G}_n$ corresponding to a prescribed boundary velocity component are equal to zero (i.e. the corresponding N^b is zero). Similarly, the constitutive equation (32) becomes,

$$\mathbf{M}_\kappa \mathbf{p}_{n+1/2} = \frac{1}{2}(\mathbf{V}_n + \mathbf{V}_{n+1} - 2\mathbf{V}_0) \ , \tag{37}$$

where the components of the volumetric mass matrix and the vector of nodal volumes are given by,

$$[\mathbf{M}_\kappa]^{ab} = \int_{V_0} \frac{1}{\kappa} N^a N^b \, dV_0 \quad ; \quad [\mathbf{V}_n]^a = \int_{V_n} N^a \, dV_n \ . \tag{38}$$

Equations (35) and (37) represent a set of nonlinear equations for the nodal pressures due to the fact that the volume vector $\mathbf{V}_{n+1}$ depends nonlinearly on the nodal positions at $n+1$ which in turn are functions of the pressure at $n+1/2$. This can solved using a standard Newton-Raphson algorithm. In order to derive the incremental equation, note first that the linearization of the nodal volumes is expressed as,

$$D\mathbf{V}^{(i)}_{n+1}[\Delta\mathbf{x}^{(i)}_{n+1}] = \mathbf{G}^{T,(i)}_{n+1} \Delta\mathbf{x}^{(i)}_{n+1} \ , \tag{39}$$

where $\Delta\mathbf{x}^{(i)}_{n+1} = \mathbf{x}^{(i+1)}_{n+1} - \mathbf{x}^{(i)}_{n+1}$ and, $\mathbf{V}^{(i)}_{n+1}$ and $\mathbf{G}^{T,(i)}_{n+1}$, are calculated from the i-th iterate of $\mathbf{x}_{n+1}$, $\mathbf{x}^{(i)}_{n+1}$. In addition, combining $\mathbf{x}_{n+1} = \mathbf{x}_n + \Delta t \, \mathbf{v}_{n+1/2}$ and the linearized form of equation (35) gives,

$$\Delta\mathbf{x}^{(i)}_{n+1} = -\frac{1}{2}\Delta t^2 \mathbf{M}^{-1}\mathbf{G}_n \Delta\mathbf{p}^{(i)}_{n+1/2} \ , \tag{40}$$

where $\Delta\mathbf{p}^{(i)}_{n+1/2} = \mathbf{p}^{(i+1)}_{n+1/2} - \mathbf{p}^{(i)}_{n+1/2}$. Equations (39) and (40) can now be combined with expression (37) to yield a Newton-Raphson iteration process for the pressure increment $\Delta\mathbf{p}^{(i)}_{n+1/2}$,

$$(\mathbf{M}_\kappa + \tfrac{1}{4}\Delta t^2 \mathbf{G}^{\mathbf{T},(i)}_{n+1}\mathbf{M}^{-1}\mathbf{G}_n)\Delta\mathbf{p}^{(i)}_{n+1/2} = \frac{1}{2}(\mathbf{V}_n + \mathbf{V}^{(i)}_{n+1} - 2\mathbf{V}_0) - \mathbf{M}_k \mathbf{p}^{(i)}_{n+1/2} \ . \tag{41}$$

The initial value for the iteration is $\mathbf{p}^{(0)}_{n+1/2} = \mathbf{p}_{n-1/2}$, and, from (35), $\mathbf{x}^{(0)}_{n+1} = \mathbf{x}_n + \Delta t \mathbf{v}^*_{n+1/2} - (\Delta t/2)\mathbf{M}^{-1}\mathbf{G}_n \mathbf{p}^{(0)}_{n+1/2}$. Note that once a new pressure increment has been computed solving the linear system (41), the geometry is easily updated using expression (40).

In the next section we present a simplified form of this algorithm will be discussed below which avoids the Newton-Raphson iteration.

For computational convenience both the mass matrix and volumetric mass matrix will be lumped. In the latter case doing this permits the direct evaluation of the nodal pressures from equation (37) to give,

$$p^a_{h,n+1/2} = \frac{\kappa}{2}(J^a_n + J^a_{n+1} - 2) \, ; \qquad J^a_n = \frac{[\mathbf{V}_n]^a}{[\mathbf{V}_0]^a} \tag{42}$$

We note that in the compressible case, it is now possible to eliminate the pressure and redefine the incremental Lagrangian in a more conventional form as a function of nodal positions alone as,

$$L_{n,n+1}(\mathbf{x}_n, \mathbf{x}_{n+1}) = \frac{1}{2}\mathbf{v}^T_{n+1/2}\mathbf{M}\mathbf{v}_{n+1/2} - \Pi_{\text{iso}}(\mathbf{x}_n) - \Pi_{\text{ext}}(\mathbf{x}_n) + \Pi_{\text{vol}}(\mathbf{x}_{n+1/2}) \tag{43}$$

where the volumetric component is,

$$\Pi_{\text{vol}}(\mathbf{x}_{n+1/2}) = \sum_{a=1}^{M} V^a_0 U(\tfrac{1}{2}J^a_n + \tfrac{1}{2}J^a_{n+1}) \, ; \qquad U(J) = \frac{1}{2}\kappa(J-1)^2 \tag{44}$$

It is easy to verify that the incremental Lagrangian (43) leads to the same set of discrete equations. Note that equation (43) can be interpreted as using the central difference form for the deviatoric component of the internal energy and a mid-point form for the volumetric energy. The resulting scheme is therefore implicit in the pressure and should have a timestep only controlled by the speed of the shear wave.

6. LINEARIZED FORMULATION

6.1. Linearization of the volume increment

The Newton-Raphson iteration that appears in the above evaluation of the nodal pressures can be eliminated if the volume increment per step is linearized. In effect, this is equivalent to the assumption that the displacements during the increment are small. This is in general a reasonable assumption to make given that the algorithms is still explicit with respect to the deviatoric component.

In order to calculate the pressure increment without the need for a Newton-Raphson iteration, consider the discretised constitutive equation (37) written in terms of the volume increment between steps as,

$$\mathbf{M}_\kappa \mathbf{p}_{n+1/2} = (\mathbf{V}_n - \mathbf{V}_0) + \frac{1}{2}\Delta\mathbf{V}_{n+1/2}\,; \qquad \Delta\mathbf{V}_{n+1/2} = \mathbf{V}_{n+1} - \mathbf{V}_n\ . \tag{45}$$

Assuming that the geometrical changes are small during the increments, the volume increment for a given node a can be expressed in terms of the divergence of the velocities as,

$$\begin{aligned} [\Delta\mathbf{V}_{n+1/2}]^a &= \int_{V_0} N^a (J_{n+1} - J_n)\, dV_0 && (46)\\ &\approx \Delta t \int_{V_n} N^a \operatorname{div} \mathbf{v}_{n+1/2}\, dV_n && (47)\\ &= \Delta t [\mathbf{G}_n^T \mathbf{v}_{n+1/2}]^a\ . && (48) \end{aligned}$$

The volumetric constitutive equation can therefore be linearized as,

$$\mathbf{M}_\kappa \mathbf{p}_{n+1/2} = (\mathbf{V}_n - \mathbf{V}_0) + \frac{\Delta t}{2}\mathbf{G}_n^T \mathbf{v}_{n+1/2}\ . \tag{49}$$

It is now possible to combine this expression with equation (35) for the mid step velocity to give a linear set of equations for the pressure as,

$$(\mathbf{M}_\kappa + \tfrac{1}{4}\Delta t^2 \mathbf{G}_n^T \mathbf{M}^{-1} \mathbf{G}_n)\mathbf{p}_{n+1/2} = (\mathbf{V}_n - \mathbf{V_0}) + \frac{\Delta t}{2}\mathbf{G}_n^T \mathbf{v}^*_{n+1/2} \tag{50}$$

The resulting time stepping algorithm can be summarized as shown in table 1.

6.2. First step

Finally it is clear that the first timestep requires special treatment, as the velocities and pressures at the previous half step are not known. (Note that the variational equilibrium equations 8 cannot be applied until two full configurations have been determined.) There are a number of ways in which this can be done, but the one which we have used and which appears

Steps:	
0.	Known : $\mathbf{x}_n$, $\mathbf{v}_{n-1/2}$, $\mathbf{p}_{n-1/2}$, $\mathbf{M}$, and $\mathbf{M}_\kappa$.
1.	Calculate $\mathbf{F}_n$, $\mathbf{T}'_n$ and $\mathbf{G}_n$.
2.	Calculate $\mathbf{v}^*_{n-1/2}$ using equation 34.
3.	Calculate $\mathbf{p}_{n+1/2}$ and using equation 50.
4.	Calculate $\mathbf{v}_{n+1/2}$ using equation 35.
5.	Calculate $\mathbf{x}_{n+1}$ using $\mathbf{x}_{n+1} = \mathbf{x}_n + \Delta t\, \mathbf{v}_{n+1/2}$.

Table I. Fractional time step algorithm

to be more natural in the context of the above algorithm is given by writing the equilibrium equation at time t_0 as,

$$\mathbf{M}\frac{\mathbf{v}^*_{1/2} - \mathbf{v}_0}{\Delta t/2} = \mathbf{F}_0 - \mathbf{T}'_0 - \frac{1}{2}\mathbf{G}_0\mathbf{p}_0 \ , \tag{51}$$

$$\mathbf{M}\frac{\mathbf{v}_{1/2} - \mathbf{v}^*_{1/2}}{\Delta t/2} = -\tfrac{1}{2}\mathbf{G}_0\mathbf{p}_{1/2} \ . \tag{52}$$

Note that if the initial configuration corresponds to the unstressed state of the body, last two terms on the right hand side of the first equation will vanish.

The above expression can be combined with the linearised constitutive equation written for the first half step as,

$$\mathbf{M}_\kappa\mathbf{p}_{1/2} = \frac{1}{2}\Delta\mathbf{V}_{1/2} \ ; \qquad \Delta\mathbf{V}_{1/2} = \mathbf{V}_1 - \mathbf{V}_0 \approx \Delta t\, \mathbf{G}_0^T\mathbf{v}_{1/2} \ , \tag{53}$$

to give a set of linear equations for the pressure values at the first half step as,

$$(\mathbf{M}_\kappa + \frac{1}{8}\Delta t^2\mathbf{G}_0^T\mathbf{M}^{-1}\mathbf{G}_0)\mathbf{p}_{1/2} = \frac{\Delta t}{2}\mathbf{G}_0^T\mathbf{v}^*_{1/2} \ . \tag{54}$$

7. LINEAR STABILITY ANALYSIS

It is clear from the previous section that the cost per step of the above algorithms is significantly greater than that of a standard explicit central difference, albeit it is still far less than a typical implicit step, which inevitably involves solving a set of highly non-linear equations for the nodal positions. The use of this type of integration will therefore only be practical if the timestep size is considerably greater than that of an explicit step. The aim of this section is to prove that the linear stability limit for the fractional scheme is governed by the speed of the sheer wave, which for nearly incompressible problems will inevitably be far slower than the pressure wave. In order to prove this, consider first the geometrical incremental Lagrangian (43) for the small displacement linear elasticity case as,

$$\begin{aligned} L_{n,n+1}(\mathbf{u}_n, \mathbf{u}_{n+1}) = \ & \frac{\Delta t}{2}\mathbf{v}^T_{n+1/2}\mathbf{M}\mathbf{v}_{n+1/2} - \Delta t\Pi_{\text{ext}}(\mathbf{u}_n) \\ & -\frac{\Delta t}{2}\mathbf{u}^T_{n+1/2}\mathbf{K}_{\text{vol}}\mathbf{u}_{n+1/2} - \frac{\Delta t}{2}\mathbf{u}^T_n\mathbf{K}_{\text{iso}}\mathbf{u}_n \end{aligned} \tag{55}$$

where as before $\mathbf{v}_{n+1/2} = (\mathbf{u}_{n+1} - \mathbf{u}_n)/\Delta t$, $\mathbf{u}$ is the vector of nodal displacements, and $\mathbf{K}_{\text{vol}}$ and $\mathbf{K}_{\text{iso}}$ represent the volumetric and isochoric (i.e. deviatoric) components of the stiffness matrix. Typically, for nearly incompressible materials $\mathbf{K}_{\text{vol}}$ will be far stiffer than $\mathbf{K}_{\text{iso}}$ and consequently it is important that it does not play a role in the evaluation of the critical timestep.
The corresponding stationary conditions lead now to the following set of linear equations,

$$\frac{1}{\Delta t^2}\mathbf{M}(\mathbf{u}_{n+1} - 2\mathbf{u}_n + \mathbf{u}_{n-1}) + \mathbf{K}_{\text{iso}}\mathbf{u}_n + \frac{1}{2}\mathbf{K}_{\text{vol}}(\mathbf{u}_{n+1/2} + \mathbf{u}_{n-1/2}) = \mathbf{F}_n \ . \tag{56}$$

The homogenous part of the above equation can be re-arranged to give,

$$\hat{\mathbf{M}}(\mathbf{u}_{n+1} + \mathbf{u}_{n-1}) + \Delta t^2(\mathbf{K} - \frac{2}{\Delta t^2}\hat{\mathbf{M}})\mathbf{u}_n = 0 \ , \tag{57}$$

where,

$$\hat{\mathbf{M}} = \mathbf{M} + \frac{4}{\Delta t^2}\mathbf{K}_{\text{vol}} \ ; \qquad \mathbf{K} = \mathbf{K}_{\text{vol}} + \mathbf{K}_{\text{iso}} \ . \tag{58}$$

Consider now the eigenvalue problem $\mathbf{K}\mathbf{w} = \lambda\hat{\mathbf{M}}\mathbf{w}$ and express the displacements as a linear combination of the corresponding eigenvectors as $\mathbf{u}_n = \sum_i r_n^i \mathbf{w}_i$. Substituting into equation (57) leads to the following difference equation for the modal components,

$$r_{n+1}^i - (2 - \lambda_i \Delta t^2) r_n^i + r_{n-1}^i = 0 \tag{59}$$

which, upon substitution of $r_n^i = A^n$, where $|A| \leq 1$ for stability, quickly leads to the standard timestep condition,

$$\Delta t \leq \frac{2}{\sqrt{\lambda_{\max}}} \tag{60}$$

In order to derive an upper bound for $\lambda_{\max}$ note that,

$$\lambda_{\max} = \max_{\mathbf{v}} \left(\frac{\mathbf{v}^T\mathbf{K}\mathbf{v}}{\mathbf{v}^T\hat{\mathbf{M}}\mathbf{v}} \right) = \max_{\mathbf{v}} \left(\frac{\mathbf{v}^T\mathbf{K}_{\text{iso}}\mathbf{v} + \mathbf{v}^T\mathbf{K}_{\text{vol}}\mathbf{v}}{\mathbf{v}^T\mathbf{M}\mathbf{v} + (\Delta t^2/4)\mathbf{v}^T\mathbf{K}_{\text{vol}}\mathbf{v}} \right) \tag{61}$$

Introducing now the maximum eigenvalue of the deviatoric stiffness component as,

$$\lambda_{\max}^{\text{iso}} = \max_{\mathbf{v}} \left(\frac{\mathbf{v}^T\mathbf{K}_{\text{iso}}\mathbf{v}}{\mathbf{v}^T\mathbf{M}\mathbf{v}} \right) \tag{62}$$

gives,

$$\lambda_{\max} \leq \max_{\mathbf{v}} \left(\frac{\lambda_{\max}^{\text{iso}}\mathbf{v}^T\mathbf{M}\mathbf{v} + (4/\Delta t^2)(\Delta t^2/4)\mathbf{v}^T\mathbf{K}_{\text{vol}}\mathbf{v}}{\mathbf{v}^T\mathbf{M}\mathbf{v} + (\Delta t^2/4)\mathbf{v}^T\mathbf{K}_{\text{vol}}\mathbf{v}} \right) \leq \max\left(\lambda_{\max}^{\text{iso}}, (4/\Delta t^2)\right) \tag{63}$$

Given that stability requires $\lambda_{max}(\Delta t^2/4) \leq 1$, the critical timestep limit is given by,

$$\Delta t \quad \leq \quad \frac{2}{\sqrt{\lambda_{\max}^{\text{iso}}}} \tag{64}$$

Thus, we see for the linear case the time step is constrained purely by the isochoric eigenvalues and is independent of the volumetric part. The fully incompressible case can either be similarly studied using the pressure as a separate independent variable or more easily as a limit case of the above derivation. The examples shown below will indicate that the stability properties

demonstrated here for the nearly incompressible linear case do in fact extend to the nonlinear and fully incompressible cases.

Finally, the maximum eigenvalue $\lambda_{\max}^{\text{iso}}$ is estimated as

$$\lambda_{\max}^{\text{iso}} = \frac{2\mu}{\rho(h_e)_{\min}^2} \ , \tag{65}$$

where $(h_e)_{\min}$, is the smallest characteristic element length over the whole mesh.

8. PRESSURE STABILIZATION

In the incompressible limit $\kappa \to \infty$, and $\mathbf{M}_k$ in equations (50) or (41) vanishes. As a result, the linear system of equations becomes singular. This can be seen by realizing that multiple solutions can be obtained by adding any vector field $\mathbf{w}$ satisfying $\mathbf{G}_n\mathbf{w} = \mathbf{0}$ to a given solution. In our implementation we choose to remedy this problem by introducing a pressure stabilization term to the discrete variational in the form:

$$\Pi_{\text{sta}}(\mathbf{p}_{n+1/2}) = \frac{1}{2}\mathbf{p}_{n+1/2}(\mathbf{M}_{\kappa^*}^L - \mathbf{M}_{\kappa^*})\mathbf{p}_{n+1/2} \ ; \qquad \kappa^* = \frac{1}{\epsilon} \tag{66}$$

where ϵ represents a small stability parameter and $\mathbf{M}_{\kappa^*}^L$ denotes the lumped version of the volumetric mass matrix $\mathbf{M}_{\kappa^*}$. It is now simple to show that the equation for the pressure (50), now becomes,

$$(\mathbf{M}_\kappa + \mathbf{M}_{\kappa^*}^L - \mathbf{M}_{\kappa^*} + \frac{1}{4}\Delta t^2 \mathbf{G}_n^T \mathbf{M}^{-1} \mathbf{G}_n)\mathbf{p}_{n+1/2} = (\mathbf{V}_n - \mathbf{V_0}) + \frac{\Delta t}{2}\mathbf{G}_n^T \mathbf{v}_{n+1/2}^*, \tag{67}$$

and equations (34) and (35) remain unchanged. The introduction of the difference between the lumped and consistent version of the volumetric mass matrix eliminates the artificial pressure modes from the system and will obviously vanish as the mesh is refined for any choice of the stability parameter ϵ.

9. EXAMPLES

9.1. A Plane Strain Case

We consider a square flat plate of unit side length under plane strain. The left and bottom boundaries were restricted to move only tangentially, whereas the top and right boundaries are restricted to move normally, as shown in figure 3. Under the assumption of small displacements, $\boldsymbol{u} = \boldsymbol{x} - \boldsymbol{X}$, the isochoric and volumetric components of the internal energy become,

$$\Pi_{\text{iso}}(\boldsymbol{u}) = \int_V \mu \boldsymbol{\epsilon}' : \boldsymbol{\epsilon}' \, dV \ ; \qquad \boldsymbol{\epsilon}' = \tfrac{1}{2}(\nabla \boldsymbol{u} + \nabla \boldsymbol{u}^T) - \tfrac{1}{3}(\operatorname{div} \boldsymbol{u})\boldsymbol{I} \tag{68}$$

$$\Pi_{\text{vol}}(\boldsymbol{u}, p) = \int_V p \operatorname{div} \boldsymbol{u} \, dV - \int_V \frac{p^2}{2\kappa} \, dV \ , \tag{69}$$

and the corresponding differential Euler-Lagrange equations can be reduced to,

$$(\lambda + \mu) \nabla (\operatorname{div} \boldsymbol{u}) + \mu \nabla^2 \boldsymbol{u} = \rho \boldsymbol{u}_{tt} \tag{70}$$

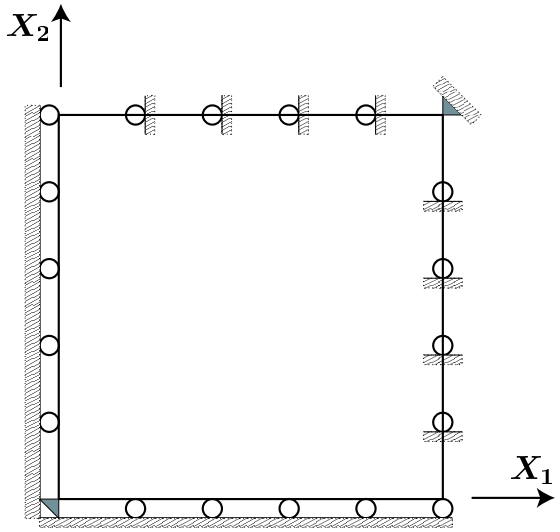

Figure 3. Two dimensional test case

where $\lambda = \kappa - \frac{2}{3}\mu$ is the standard Lame coefficient. An analytical solution for this problem is easily obtained. In particular, with the appropriate choice of initial condition the solution becomes, $(c_d = \sqrt{\frac{\mu}{\rho}})$

$$\boldsymbol{u}(t) = U_0 \cos(\frac{c_d \pi t}{2}) \begin{bmatrix} \sin\left(\frac{\pi X_1}{2}\right) \cos\left(\frac{\pi X_2}{2}\right) \\ -\cos\left(\frac{\pi X_1}{2}\right) \sin\left(\frac{\pi X_2}{2}\right) \end{bmatrix} . \tag{71}$$

Note that this solution is only a function of μ, and is independent of the compressibility of the material. In order to test our formulation, we have discretized the domain into 288 equal triangles, and run this problem with the fractional step algorithm proposed with a non-linear Neo-Hookean material as well as with the linearized small displacement potentials given by equations (68, 69). For values of U_0 below 0.001 we have found no appreciable difference in the computed solutions.

Figure 4 shows the displacement of the point at $X_1 = 1$, $X_2 = 0$ versus the non-dimensional time, compared to the analytical solution. In this case the code was run assuming nearly incompressibility for a value of $\kappa/\mu = 5000$, which corresponds to a Poisson's ratio of $\nu = (1 - \mu/\kappa)/2 = 0.4999$. The agreement with the analytical solution is excellent. We note that if this problem had been run with an explicit code, the timestep would have been of the order of $\Delta t \sim (h_e)_{\min}/\sqrt{(\lambda + 2\mu)/\rho}$ which would have been about 35 times smaller than the timestep used in the calculation. Figure 5 shows the same calculation but now for a totally incompressible material $\nu = 0.5$. This case could not be run with an explicit code as, in this case, the size of the allowable timestep would go to zero. We note that the results are undistinguishable from the previous nearly incompressible case, as expected. Finally, figure 6 depicts the time history of the normalized total energy, E, showing also the contribution from the kinetic, $M(\boldsymbol{v}_{n+1/2}, \boldsymbol{v}_{n+1/2})/2$, and potential $\Pi_{\text{iso}}(\boldsymbol{x}_n) + \Pi_{\text{ext}}(\boldsymbol{x}_n)$ components. Here, the potential energy due to volumetric deformation is equal to zero. It is clear that since the

external forces do not do any work, the total energy should be conserved. Numerically we observe a small oscillation about the conserved value which, obviously, decreases when the discretization is refined. Nevertheless, the average level of the total energy does not decay but stays constant.

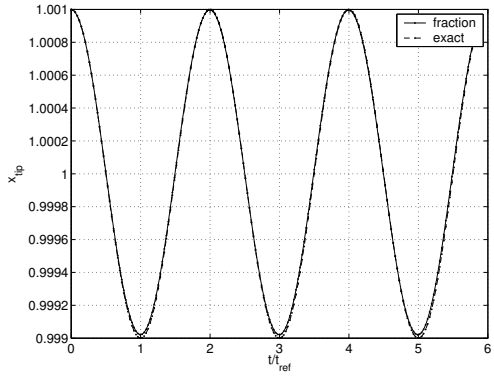

Figure 4. Displacement of point $X_1 = 1$, $X_2 = 0$ in time for nearly incompressible solution ($\nu = 0.4999$) compared with analytical solution.

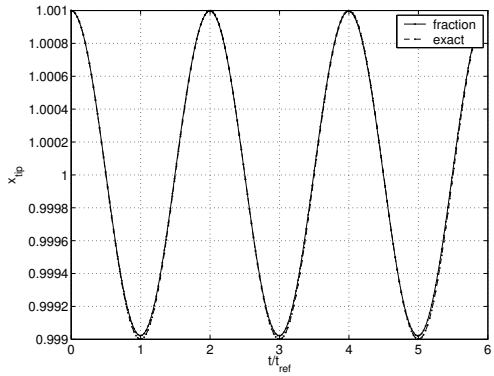

Figure 5. Displacement of point $X_1 = 1$, $X_2 = 0$ in time for incompressible solution ($\nu = 0.5$) compared with analytical solution.

9.2. A spinning plate

A unit thickness square plate without any constraints is released without any initial deformation and an initial angular velocity of 1 rad/s, figure 7. This problem is chosen to illustrate the conservation properties of fractional time stepping algorithm proposed. The density of the plate and edge length are chosen to be unity. The Young's modulus given by, $3\mu/(1 + \mu/(3\kappa))$ was chosen to be unity and the Poisson's ratio, $(1 - \mu/\kappa)/2$, was 0.45. The plate was meshed with 288 equal linear triangular elements as shown in figure 8, which also shows the levels of the pressure distribution (although shown constant over each element for display purposes, the pressure is continuous and has a linear variation over each element). Given that the center of mass is initially at zero velocity, we expect it to remain so. In addition, we expect the angular momentum, $\int_{V_0} \boldsymbol{x}_{n+1} \times \boldsymbol{v}_{n+1/2} \rho_0 \, dV_0$, to stay constant at its initial value.

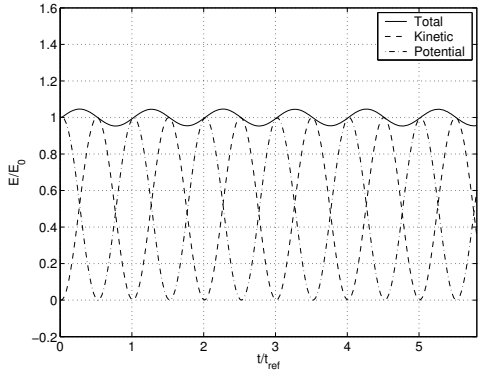

Figure 6. Energy History.

The time history of the linear and angular momentum are shown in figure 9. Note that the initial conditions used here are such that there is no steady state solution, even in a rotating reference frame.

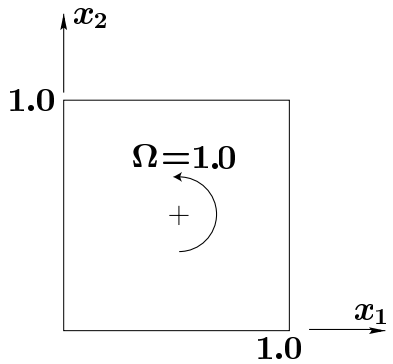

Figure 7. Spinning plate test case.

9.3. 2D Beam bending

The bottom side of a unit thickness beam, moving at a constant velocity $V_0 = 0.1$, is instantly brought to rest as shown in figure 10. The density of the material of the beam, its Young's modulus, and the width of the beam are chosen to be unity. The Poisson's ratio, $(1-\mu/\kappa)/2$ of the material is 0.45 and the length of the beam is taken to be 6.0. This problem is non-linear and involves large deformations. The beam is was meshed with linear triangular elements as shown in figure 11 where the pressure distribution at a given time during the simulation is also shown.

For this problem we show the time evolution of the energy in figure 12. Here, the potential energy is given by $\Pi_{\text{iso}}(\boldsymbol{x}_n) + \Pi_{\text{ext}}(\boldsymbol{x}_n) + \int_{V_0}(p_{n+1}/2)(J_{n+1} + J_n - 2)\, dV_0 - \int_{V_0}(p_{n+1}^2/2\kappa)\, dV_0$. Numerically, we see that the energy oscillates about the exact constant value. Again, we note that the scheme is not dissipative and therefore very well suited for long time integrations.

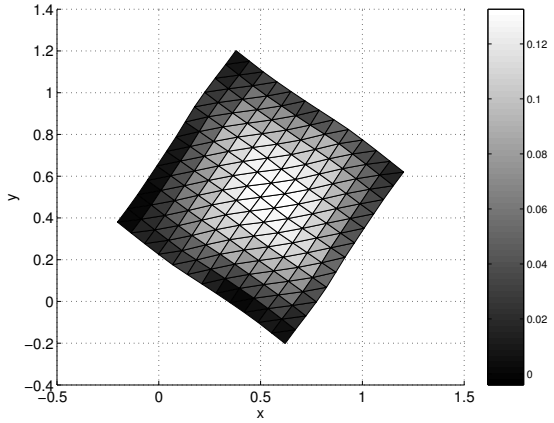

Figure 8. Finite element mesh and pressure distribution at a given instant.

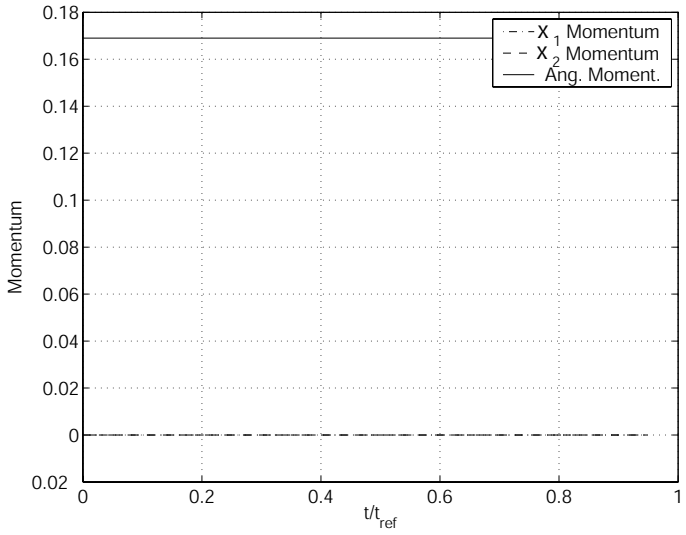

Figure 9. Linear momentum and angular momentum plots.

9.4. 3D Cylinder Bending

A final three dimensional example is presented in this section. This involves a similar bending problem to that discussed in the previous section. A half cylinder travelling with uniform speed has its base suddenly fixed thus leading to a large strain oscillatory motion. The initial radius of the cylinder is 0.32 m, its length 3.24 m and the initial speed is 2.42 m/s. This set of data correspond to the example already discussed in reference [14]. The initial mesh is shown in figure 13 which also illustrates the deformed configuration after 5 seconds. In order to demonstrate that the allowable timestep is still independent of the bulk modulus, the problem has been re-run with increasing κ/μ ratios. The resulting allowable timestep, normalized by

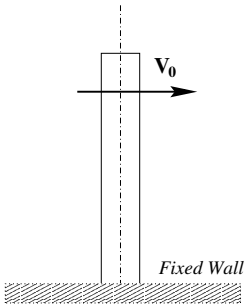

Figure 10. Beam bending

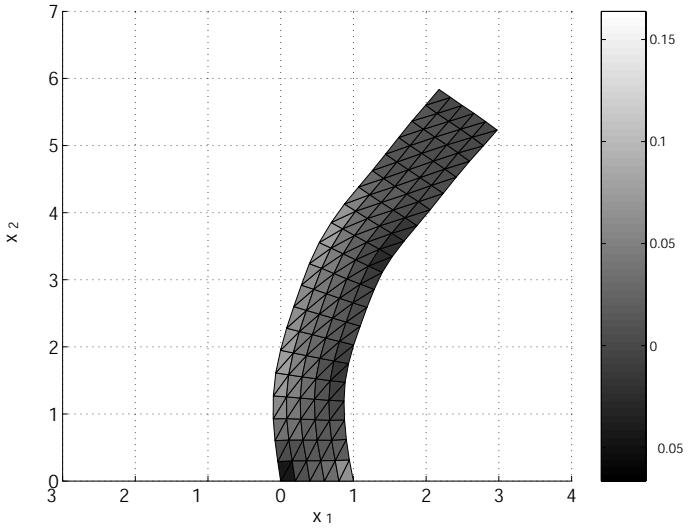

Figure 11. Pressure distribution in the beam.

the allowable timestep of the standard explict scheme when $\kappa/\mu = 1$, is shown in figure 14 which clearly illustrates the desired behavior.

10. CONCLUDING REMARKS

We have described a fractional step algorithm for the simulation of dynamic problems involving incompressible or nearly incompressible material. The method has a variational interpretation and it can be easily shown to conserve exactly linear and angular momentum. In addition the method possesses excellent energy conservation properties which makes it well suited for long time integrations. The method requires the solution of a symmetric Poisson-like equation at each timestep for the pressure variable. This is clearly much cheaper than a fully implicit scheme requiring the solution of a non-symmetric system of equations involving three times as

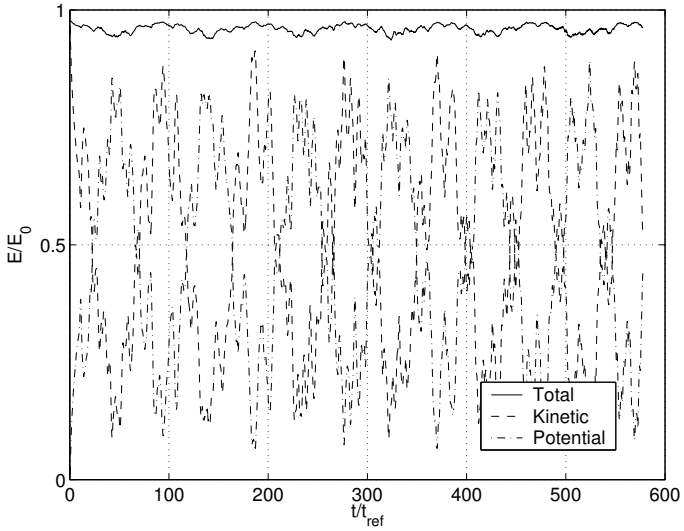

Figure 12. Energy fluctuations in the case of fractional method.

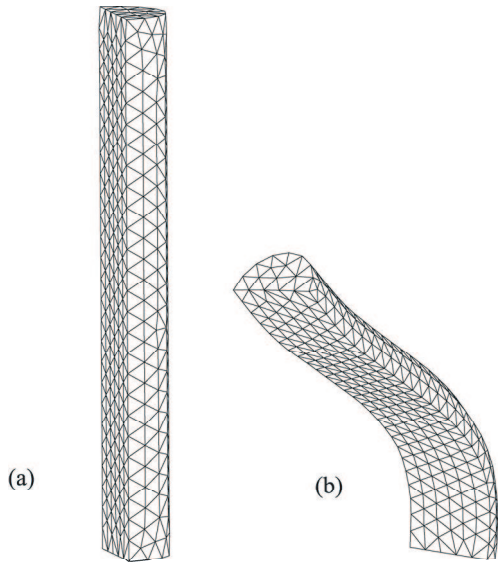

Figure 13. 3-D bending example. (a) Initial mesh; (b) deformed configuration

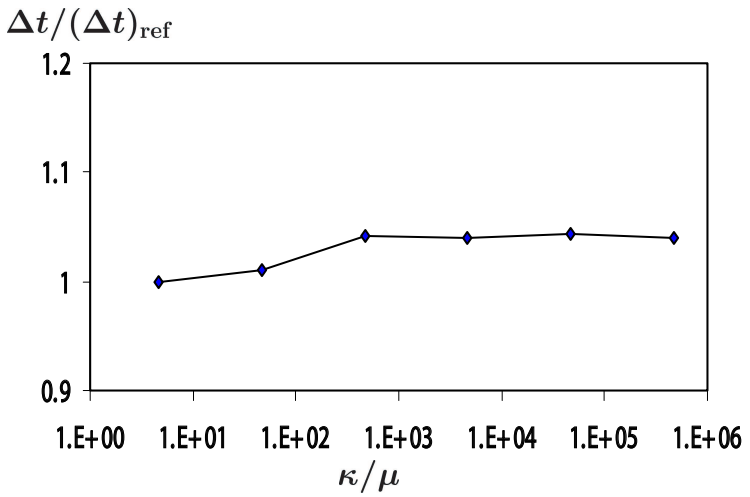

Figure 14. Dependency of maximum stable timestep on bulk modulus (3-D example)

many unknowns (in 3D). For large values of κ, the timestep size of the presented method is approximately $(\sqrt{3}/2)(\sqrt{\kappa/\mu})$ times larger than the timestep of the standard explicit scheme. Further work is clearly needed in order to assess the range of problems for which the extra cost induced by the fractional step method is compensated by the larger step size permitted. For the presented algorithm the linearized analysis shows that the timestep should be independent of κ and this is confirmed by our computations in the linear and the non-linear regimes.

ACKNOWLEDGEMENT

This work has been funded by Sandia National Laboratories, USA., through a collaborative research contract with MIT (Doc. No. 1152 under A0260). The authors wish to thank Dr. James R. Stewart, from Sandia National Laboratories and Professor Raul Radovitsky from Department of Aeronautics and Astronautics, MIT, for the research interactions and collaboration.

REFERENCES

1. Newmark N. M. A method of computation for structural dynamics *ASCE Journal of Engineering Mechanics Division* (1959):67–94.
2. Ortiz M. A note on energy conservation and stability of nonlinear time-stepping algorithms. *Computers and Structures* **24**(1986):167-168
3. Wendlandt J. and Marsden J. E. Mechanical integrators derived from a discrete variational principle *Physica D* **106**(1997):223–246.
4. Kane C., Marsden J. E., Ortiz M., West M. Variational integrators and the Newmark algorithm for conservative and dissipative mechanical systems *Int. J. Num. Meth. Engrg.* **49**(2000):1295–1325.
5. Marsden J. E., Pekarsky S. and Shkoller S. Discrete Euler-Poincaré and Lie-Poisson equations *Nonlinearity* **12**(1999):1647–1662.
6. Simo J. C., Tarnow N., Wong K. K. Exact energy-momentum conserving algorithms and symplectic schemes for nonlinear dynamics. *Comp. Meth. in Appl. Mech. and Engrg.* **100**(1992):63-116
7. Simo J. C., Tarnow N. The discrete energy momentum integrators. Conserving algorithms for nonlinear elastodynamics. *Zietschrift fuer Argewandte Mathematik und Physik* **43**(1992):757–792

8. Simo J. C., Gonzalez O. Assessment of of energy-momentum and symplectic schemes for stiff dynamical systems *Proceesings of ASME Winter Annual Meeting, New Orleans* (December 1996)
9. Veselov A.P. Integrable discrete-time systems and difference operators. *Functional Analysis and its Applications* **22**(1988):83-94
10. Chorin A. J. Numerical solution of the Navier-Stokes equations. *Math. Comput.* 1991; **22**(1968):745–762.
11. Bonet J. and Burton A. J. A simple averaged nodal pressure tetrahedral element for nearly incompressible dynamic explicit applications. *Comm. Num. Meth. Engrg.* 1998; **14**(1998):437–449.
12. Zienkiewicz O. C., Rojek J., Taylor R. L., Pastor M. Triangles and tetrahedra in explicit dynamic codes for solids *Int. J. Num. Meth. Engrg.* **43**(1998):565–583.
13. Bonet J., Marriott H., Hassan O. Stability and comparison of different linear tetrahedral formulations for nearly incompressible explicit dynamic applications *Int. J. Num. Meth. Engrg.* **50**(2001):119–133.
14. Bonet J., Marriott H., Hassan O. An averaged nodal deformation gradient linear tetrahedral element for large strain explicit dynamic applications *Comm. Num. Meth. Engrg.* **17**(2001):551–561.
15. Gonzalez O. Time integration and Discrete Hamiltonian systems *Journal of Nonlinear Science* **6**(1996):449–469.
16. Gonzalez O., Simo J. C. On the stability of symplectic and energy-momentum algorithms for non-linear Hamiltonian systems with symmetry. *Comp. Meth. in Appl. Mech. Engrg.* **134(3-4)**(1996):197–222.
17. Armero F., Simo J. C. A-priori stability estimates and unconditionally stable product formula algorithms for non-linear coupled thermoplasticity. *International Journal of Plasticity* **9**(1993):149–182.
18. Armero F., Simo J. C. Formulation of a new class of fractional step methods for the incompressible MHD equations that retains the long-term dissipativity of the continuum dynamical system. *Fields Institute of Communications* **10**(1996):1–23.
19. Marsden J.E., Hughes T.J.R., Mathematical Foundations of Elasticity, Dover, 1983.

